New Effective Method for Quantitative Analysis of Diffusion Jumps, Applied in Molecular Dynamics Simulations of Small Molecules Dispersed in Short Chain Systems

Theophanes E. Raptis,[†] Vasilios E. Raptis,[‡] and Jannis Samios*[,§]

Division of Applied Technology, National Centre of Scientific Research "Demokritos" 153 10 Athens, Greece, Department of Chemistry, University of Ioannina 451 10 Ioannina, Greece, and Department of Chemistry, Laboratory of Physical and Theoretical Chemistry, University of Athens, Panepistimiopolis 157 71, Athens, Greece

Received: April 16, 2007; In Final Form: July 21, 2007

Diffusion jumps of small molecules dispersed in chain molecules or other kinds of slow-moving matrices have already been observed in many previous simulations of such systems, and their treatment led to important qualitative conclusions. In the present work, a new, very simple yet effective method is described, allowing for both identification of individual penetrant jump events and their quantitative treatment in a statistical sense. The method is applied in equilibrium Molecular Dynamics simulations for systems of gaseous alkanes, methane through *n*-butane, including also a mixture of methane and *n*-butane, dispersed in *n*-decane or *n*-eicosane. Equilibration and attainment of a linear diffusion regime is confirmed by means of various criteria, and the jumps detection method is applied to all systems studied. The results obtained clearly show the existence of distinct jump events in all cases, although the average jump length is reduced with penetrant or liquid alkane molecular weight. The method allows one to determine the average jump length and the corresponding jumps frequency. On the basis of these results, it was possible to estimate a random walk type diffusion coefficient, $D_{s,jumps}$, of the penetrants, which was found to be substantially lower compared with the overall diffusion coefficient $D_{s,MSD}$ obtained by the mean square displacement method. This finding led us to assume that the overall penetrants' diffusion in the studied systems is a combination of longer jumps with a smoother and more gradual displacement, a result that confirms assumptions suggested in previous studies.

1. Introduction

Jumps of small diffusing molecules play an important role in diffusion theory. Although the concept of diffusion jump is a highly idealized one, it constitutes a theoretically appealing notion since it has strong similarities to the random walk model. Diffusion in molecular liquids is considered to proceed via such small random translocations of a molecule hopping from a "cage" formed by its nearest neighbor to a nearby empty site generated as a result of thermal fluctuations.[1] A rather different situation occurs as we move on to more or less fixed matrices, such as those formed by high molecular weight chains, with small molecules dispersed therein. In these systems, free volume cavities may exist for long time scales as compared with thermal fluctuations duration, but at the same time, they are situated relatively far apart, thus leading to infrequent and longer penetrant translocations, as the literature cited in the next paragraphs shows. Such events are actually complicated sequences of translations combined with intramolecular rearrangements rather than more or less sudden events as those referred to within the framework of molecular liquid systems. However, the penetrant molecules are trapped in cavities for relatively long time scales, so that a penetrant moving to another free volume site comes up as a comparatively sharp process, thus justifying its characterization as a jump.

Nowadays, it is generally assumed that diffusion of small molecules in polymer matrices often, but not uniquely, proceeds through such a "hopping mechanism" of diffusive jumps. These jumps can be directly observed by analyzing trajectories obtained within the framework of computer atomistic simulations. Numerous examples of such observations exist in the literature, usually visualized in the form of diagrams depicting the distance of a single molecule from its initial position versus time or as two- or three-dimensional pictures of penetrant's successive positions, of course after removing periodic boundary conditions.

In this work, we are interested in the diffusion of small molecules through slowly moving "matrices", such as chain molecules or other kinds of systems. With respect to the nature of the matrix wherein penetrants diffuse, we may distinguish three broad classes of systems: ordered fixed matrices, disordered fixed matrices, and "dynamic" amorphous systems. The term "fixed" used in the first two cases should not be interpreted in an absolute sense; it merely denotes the persistence of a basic structural pattern that thermal fluctuations or penetrants' motion cannot destroy. Crystals and zeolites are typical representatives of the first class. Their order is reflected upon the regular spatial arrangement of the interstitial sites where a penetrant molecule can jump in. This regularity allows one to study diffusion by simply assuming a model based on the probability of jumps from a given site to each of the adjacent ones. In the case of zeolite systems, transition state theory (TST) has also been applied, and abundant literature exists on the topic (see, for example, refs 2−10). These approaches actually represent the

* Corresponding author. Phone: +3021−0727−4534. E-mail: isamios@chem.uoa.gr.
[†] National Centre of Scientific Research.
[‡] University of Ioannina.
[§] University of Athens.

10.1021/jp0729415 CCC: $37.00
Published on Web 11/03/2007

inverse one with respect to ours, that is, the ad hoc assumption of a jump driven diffusion mechanism.

A rather different situation occurs in the second class, the one of amorphous fixed matrices. Glassy polymers and other similar systems belong to this class. In such systems, holes or vacant sites are not located in space in a regular manner but rather randomly. The procedure usually applied is that of creating samples based on reliable atomistic models and then generating a detailed map of the voids, based on either free volume analysis or potential energy surface considerations; in the latter case, penetrant "macrostates" are identified as the union of adjacent possible penetrant locations with low potential energy separated by very low (smaller than k_BT) energy barriers. Then, the network of paths formed by possible jumps to nearby cavities or macrostates is considered; TST is employed to estimate the rate of transition from one node of the network to another, and subsequent statistical analysis allows one to estimate the diffusivity. Again, numerous works exist in this area.[11−19] The feature in common with the analysis of systems falling in the first class is the assumption of a jump diffusion mechanism prevailing on all other possibilities. It should be mentioned here that systems belonging to the last two classes are characterized by very slow dynamics and direct observation of diffusion by means of the molecular dynamics (MD) technique is quite difficult, as it usually requires time-consuming simulations.

Finally, in the third category, one may deal with such systems as rubbery macromolecular ones. The matrices through which penetrants diffuse, change with time, and their dynamics are characterized by a vast spectrum of time scales. Local rearrangements allow for free volume cavities to appear and disappear, change their shape and position, merge, or split. At the same time, deformation of the matrix may allow for a penetrant to move smoothly rather than suddenly from one site to another, so that jumps do not constitute the only cause of diffusion but may coexist with other microscopic mechanisms as well. It is in such systems that MD applies for the study of diffusion processes, and penetrant jumps may be directly observed. On the other hand, the rather fast dynamics of free volume do not allow one to apply such techniques as TST, which are based on the a priori knowledge of the free volume cavities position, so that MD is the common option.

Numerous treatments of such systems[20−42] imply that one can easily identify jumps as abrupt changes in a plot of displacement versus time or as "threads" connecting highly populated regions in three-dimensional graphs of penetrant positions. These methods do provide a picture of penetrant jumps that take place, although they do not constitute a rigorous definition of what is a jump. On the other hand, attempts to derive a method for a quantitative treatment of jumps are characterized by a certain arbitrariness in the form of varying parameters that cannot be determined in any other way but by comparison with mean square displacement data, except in ref 30 where local orientation correlation functions were used to devise a spectrum of characteristic length scales. However, using mean square displacement data to tune arbitrary parameters of the jump models is in general incorrect, since microscopic mechanisms other than the hopping one have been observed in numerous cases. It is worth noting, for instance, the work of Hahn et al.[32] in which it is suggested that, in the case of phenol molecules in bisphenol A-polycarbonate, diffusion mechanisms other than the usually postulated one of jumps are the main contributors to the overall diffusive motion. Instead of more or less fixed cavities whose volume may fluctuate but their location is essentially constant throughout the simulation, they observed a certain coupling of penetrant and local polymer motion resulting in the penetrant carrying the necessary free volume like a turtle carries its shell, thus leading to a continuous rather than hopping form of translocation.

Given the above, researchers often lean toward using plots of displacement versus time as a handy tool to treat the jumps observed in a quantitative manner.[21,22,24−26,32−35,40] This is problematic, however, since this kind of representation is characterized by its inability to take into account the direction in space a penetrant moves toward. Indeed, a molecular jump may be considered as a combination of longitudinal and transverse displacements with respect to the line connecting the original and current penetrant position. A purely longitudinal jump would be correctly identified quantitatively, whereas a transverse one would hardly show up in the graph. In the simple but illustrative scenario of a molecule jumping between different points on a spherical surface centered at a position defined as initial, the respective jumps would be severely underestimated. Furthermore, as the molecule diffuses away from its original position, all such "transverse" jumps would be virtually indistinguishable from thermal noise in a plot of displacement with time. Therefore, the underestimation effect in such representations seems to be more apparent with increasing time. Of course, the displacement can be defined not only as a function of distance but also as a function of x, y, or z. However, such data sets are in general too "noisy" and need additional processing and filtering before proceeding to further statistical treatment.

In this work, we present a new alternative for a precise identification of the diffusion jumps. The method has been successfully applied to a number of systems consisting of small gaseous alkane particles diffusing through similar linear molecules of higher molecular weight. It is based on tracking the size of the region occupied by a specific number of successive penetrant positions, throughout the simulation. In this way, one can identify all isolated jumps and determine the respective jump lengths. This kind of data can be further statistically processed leading to information concerning both the average jump length and the frequency of hopping events, provided that a large enough sample has been obtained. With the aid of this information, one can clarify the extent of jumps contribution to the overall diffusion and thus to elucidate the possible microscopic mechanisms underlying the behavior of diffusion processes in such systems. Finally, it should be noted that the proposed approach is capable of detecting the jump events regardless of their origin, that is, whether the penetrant escaped from a cavity and moved to another one or whether it was suddenly drawn away because of the matrix's structural rearrangement or other collective motion.

The present work is organized as follows: In section 2, we describe the systems studied, the employed simulation methodology, as well as the principles and details of the new jumps detection method. In section 3, the simulation results are presented and discussed. In particular, the simulation trajectory data are processed, and information on the jump statistics is obtained and analyzed via our new method. A summary of the main results of our treatment is given in section 4.

Finally, in Appendix A, we justify a specific subset of the potential parameters to model the liquid alkanes and penetrant molecules. In Appendix B, some necessary mathematical manipulations are presented in order to clarify specific parts of the argumentation in the main text.

TABLE 1: Atomistic United Atom Force Field Used in the Simulations

bonded interactions	stretching: $V_l = \frac{1}{2} k_l (l - l_0)^2$		
	bending: $V_\theta = \frac{1}{2} k_l (\theta - \theta_0)^2$		
	torsion: $V_\phi = \frac{1}{2} k_\phi (1 + \cos 3\phi)$		
nonbonded interactions	local interactions: of the same functional form as nonlocal ones		
	$V_{nb} = 4\epsilon_{ij}\left(\left(\frac{\sigma_{ij}}{r_{ij}}\right)^{12} - \left(\frac{\sigma_{ij}}{r_{ij}}\right)^{6}\right)$ nonlocal interactions		
		C−C	l_0 (Å) 1.54
			k_l (kcal mol^{-1}Å^{-2}) 192
		C−C−C	θ_0 (°) 114
			k_θ (kcal mol^{-1} rad^{-2}) 124.2
		C−C	k_φ (kcal mol^{-1}) 3.25
		CH_2	σ (Å) 3.53
			ϵ (kcal mol^{-1}) 0.026
		CH_3	σ (Å) 3.53
			ϵ (kcal mol^{-1}) 0.026
		CH_2	σ (Å) 3.95
			ϵ (kcal mol^{-1}) 0.091
		CH_3	σ (Å) 3.75
			ϵ (kcal mol^{-1}) 0.195
		CH_4	σ (Å) 3.73
			ϵ (kcal mol^{-1}) 0.294

2. Fundamentals

2.1. Simulation Details. Systems consisting of gaseous alkanes dispersed in higher molecular weight normal alkanes were simulated by means of the equilibrium MD simulation technique. In particular, we studied the diffusion of methane, ethane, propane, and *n*-butane, as well as that of an equimolecular mixture of methane and *n*-butane, in linear hydrocarbons of the type C_nH_{2n+2}, $n = 10, 20$, hereafter referred to as "heavy substances" or "liquids". The penetrant gases are chemically similar to the heavier substances, and therefore, interference by other factors such as molecular architecture and chemical composition is almost eliminated. The effect of such factors on jumps statistics, microscopic mass transport mechanisms, and other aspects of diffusion processes will be dealt with in forthcoming studies. Normal pressure and ambient temperature were chosen as conditions for all simulations, as will be explained in the following subsections.

Force Field. Several united atom models exist in the literature, which can reliably describe alkane molecules. Taking this into account, a similar representation has been adopted here, in which both CH_2 and CH_3 groups are represented as unified interaction centers. The model used in this study is based on the well-known NERD[43] and UA−TraPPE[44] models, which have been successfully used in simulations of the homologous series of alkanes. The modified NERD/UA−TraPPE force field, introduced in this work and hereafter referred to as mNT, accounts for a torsional potential combined with "local" or short range nonbonded interactions. Separating the intrinsic bond torsion potentials from the influence of nearby interaction sites will allow us to study the effect of molecule rigidity, architecture, and other factors in a systematic manner.

In mNT, the torsional potential is given as the sum of simple torsion terms of the form:

$$V_\phi = \frac{1}{2} k_\phi (1 + \cos 3\phi) \tag{1}$$

In eq 1, φ stands for a dihedral angle defined by four consecutive atoms along the molecular chain. The "local" nonbonded potential acts between sites belonging to the same molecule and is separated by three or four bonds. It is a sum of terms characterized by their own parameters, σ_{ij} and ϵ_{ij}, for a 12-6 Lennard-Jones, LJ, potential,

$$V_{nb} = 4\epsilon_{ij}\left(\left(\frac{\sigma_{ij}}{r_{ij}}\right)^{12} - \left(\frac{\sigma_{ij}}{r_{ij}}\right)^{6}\right) \tag{2}$$

where r_{ij} is the distance between two united atoms *i* and *j*. It is assumed that these local interactions contribute to the torsion potential, while they have no significant influence on the thermodynamic properties. The latter are mainly affected by the "nonlocal" interactions, that is, the rest of the nonbonded interactions, which are characterized by the usual UA−TraPPE parameters involved in similar energy contributions of the form of eq 2.

Within the mNT model, bonds are flexible and obey a quadratic potential. The corresponding mNT parameters were obtained from the NERD potential. All mNT parameters are summarized in Table 1. A further discussion on the determination of the exact values for the parameters can be found in Appendix A.

Systems Construction. In each case, the initial configuration was constructed at a density equal to that of the pure heavy alkane, at a given temperature and pressure. All such structures contained 1000 united atoms of the heavy substance, so that for every C_nH_{2n+2} system the number of heavy substance molecules was 1000/*n*. Every mixture contained 20 penetrant molecules of the diffusing substance (methane or butane) except in the case of a methane−butane mixture in which, 10 molecules of each gaseous alkane were present. Hence, the corresponding heavy substance gas mixtures contained 1020, 1040, 1060, 1080, or 1050 united atoms, for the cases of methane through *n*-butane and of the methane/butane mixture, respectively. The penetrants were uniformly dispersed in the systems, thanks to the sample construction method, as explained in the next paragraph. This fact was confirmed by inspecting their positions in the samples.

The creation of the initial configuration for each system was a two-step process. In the first step, all heavy substance and gaseous molecules were built in parallel; that is, a new bond was added at each step of the calculation for each molecule. Trial bond orientations were accepted or rejected using a Metropolis criterion that involved the sum of torsion and local nonbonded energy due to the new bond addition. All angles and bonds were taken to be at their equilibrium values, while the equivalent atomic diameter was taken to be 2.5 Å. Configurations with a strong overlap between nonbonded pairs, that is, for a pair distance lower than $0.7\sigma_{ij}$, were excluded. This procedure allows for a very fast construction of initial configurations with reasonable dihedral angles distributions. At this stage, no other nonlocal Lennard−Jones interactions were taken into account. Cubic periodic boundary conditions were imposed, and the simulation cell dimensions were determined according to the desired initial density.

In the second step, a simple Monte Carlo, MC, scheme was employed in order to perform energy optimization. Small

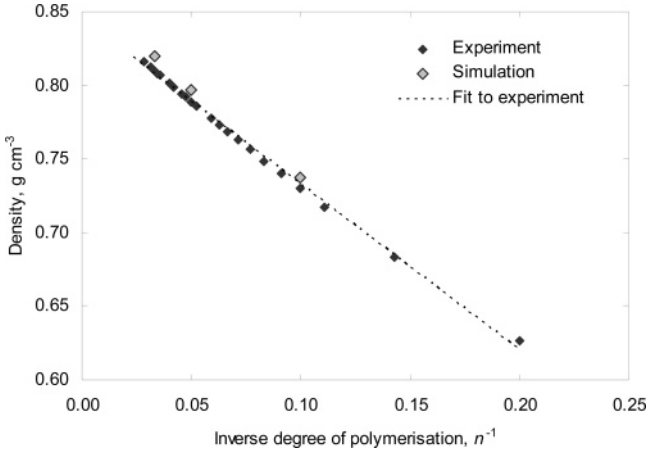

Figure 1. Pure normal alkanes, $n-C_nH_{2n+2}$, density (g cm^{-3}) at 293.15 K temperature and normal pressure with respect to inverse degree of polymerization, n^{-1}: simulation and experimental values.

displacements of randomly selected atoms constituted the MC moves used at this stage. Here, the full potential was used, and variation of all internal coordinates was allowed. This process was employed in a series of consecutive MC cycles with gradually increasing atomic diameters up to their normal values given by our model. The number of moves per cycle varied from 10^5 to 5×10^5, depending on the speed by which energy approached a minimum. The structure, relaxed during each cycle, was used as input to the next calculation with larger atomic diameters. Apart from relaxation toward a lower energy state, the scope of this stage was a gradual decorrelation of the initial configuration by lifting all constraints from bonds and angles so as to have a more natural structure as a starting point. A basic criterion providing such evidence was the attainment of smooth and diffuse bond angles and dihedral angles distributions with respect to the chain molecules, instead of the discrete ones imposed during the first stage.[45] Finally, the density was held constant throughout the second stage, as well.

Molecular Dynamics Details. MD simulations have been performed in the isothermal−isobaric, NPT, statistical mechanical ensemble, at normal pressure and 293.15 K temperature, which correspond to experimental values for the pure alkanes densities.[46] Apart from the liquid−gas mixtures under study, simulations were also performed with three structures of pure *n*-decane, *n*-eicosane, and *n*-triacontane under the same conditions. The simulated densities were found to exceed the experimental values at about 0.5−1%, which are found to be in good agreement with experiment. In Figure 1, we present a direct comparison between experimental values of densities at various molecular weights and those obtained from our simulation at 293.15 K.

In all MD simulations of pure heavy substance and gas mixtures, we utilized a fifth order Gear predictor-corrector algorithm[47] with a time step of 0.5 fs. Cubic periodic boundary conditions were applied, and the Verlet neighbor list technique[48] was also employed for speeding up calculations of nonbonded interactions. A cutoff distance of 2.33 σ_{ij}, where σ_{ij} denotes the equivalent diameter of the *ij* atom pair, was adopted for the LJ potential. At distances greater than 1.45 σ_{ij}, the LJ potential was approximated by a fifth order spline polynomial in order to eliminate discontinuities at the cutoff distance. All simulations were performed with the Nosé−Klein method for the NPT ensemble.[49] Application of this method required the calculation of the energy and pressure correction due to the applied cutoff of nonbonded potential, which accounted for the interactions at greater distances. Pressure calculation involved computation of the instantaneous molecular virial,[50] which is exclusively formed by intermolecular nonbonded contributions and is, therefore, computationally less demanding. All simulations lasted for 6 ns of which the first one was taken as an equilibration stage.

Prior to the analysis of the mass transport phenomena, certain criteria were employed to assess the initial structures and corresponding MD trajectories obtained, especially in terms of sufficient equilibration. The total potential energy and its components, namely, stretching, bending, torsion, and Lennard-Jones energy, were recorded. It was observed that total and nonbonded energy decreased during the first 50 to 100 ps and from then on kept fluctuating about a constant value. The other components also exhibited the same fluctuating behavior from the beginning. This is an indication that residual overlaps among the various interaction sites, which escaped the equilibration stage during the initial structure generation process, were easily removed during the MD simulation. The running average of the systems density was also recorded, and it was observed to reach an asymptotic value within the first 1 ns of the simulations. To check whether the systems were homogeneous, the simulation box was divided in eight equal sub-boxes, and the number density running average in each of them was recorded. It was observed that the density of each sub-box and that of the whole box practically coincided within the first 1 ns equilibration period.

The dihedral angles distribution of the initial structures was computed and compared to the average distribution obtained during each nanosecond (ns) of the simulations. It was found that the distribution remained practically the same as a result of the building procedure which ensures the generation of amorphous structures. On the other hand, time autocorrelation in the form of first and second order Legendre polynomials, of the end-to-end vector of whole chains and subchains of various lengths, clearly showed mobility and loss of structural memory.[45] Thus, the systems were not frozen in their initial state but were actually liquid.

2.2. Proposed Jumps Detection Method: Diffusion Mechanisms. As mentioned above and following the literature so far, jumps are usually identified by previous workers as more or less abrupt changes observed in graphs of a single molecule's displacement with respect to its initial position. The true molecular motion is not always described correctly by such graphs, since the translating molecule may jump between sites that are situated at roughly equal distances from the penetrant's initial position. Because of this fact, contribution of the jump mechanism might appear to be underestimated. On the other hand, detailed information concerning the jumps distribution might be quite helpful in order to understand more precisely the mass transport processes. In an effort to elucidate the contribution of the different diffusion mechanisms in the framework of our simulations, devise improved tools for presenting the penetrant translation information, and clarify the diffusive jump notion itself, we employ a new quantitative method, which is described herein.

According to it, we accept that the penetrant molecule spends most of its time being trapped inside various free volume cavities formed by the heavy substance molecules. Thus, by recording its center-of-mass position *N* times within a time interval Δt, it is most probable to collect a cloud or swarm of points concentrated inside a particular area. From time to time, thermal

fluctuations allow the penetrant to pass from one cavity to another. If such a jump event occurs during the observation time interval Δt, the swarm of points should become elongated. Of course, a similar effect is to be expected in the case of a penetrant moving from one end of an elongated cavity to the other. In the present approach, we are not concerned with the polymeric environment but rather with the penetrant trajectory itself.

By taking into account an appropriate measure of the swarm size as a function of time, one expects to observe a number of peaks corresponding to the occurrence of particular jumps. Such a measure can be given in terms of the radius of gyration, R_G, taken over all swarm points

$$R_G(t;\Delta t) = \sqrt{\frac{1}{N}\sum_{i=1}^{N}(\mathbf{R}_i(t;\Delta t) - \mathbf{R}_{CM}(t;\Delta t))^2} \qquad (3)$$

where time t denotes the middle of observation time interval Δt, $\mathbf{R}_i(t;\Delta t) = \mathbf{R}(t - \Delta t/2 + i\Delta t/N)$ is the position of every observation point and $\mathbf{R}_{CM}$ is the swarm center of mass, defined as follows:

$$\mathbf{R}_{CM} = \frac{1}{N}\sum_{i=1}^{N}\mathbf{R}_i(t;\Delta t) \qquad (4)$$

By using such a criterion, we define jump length $\lambda'(t;\Delta t)$ by the following relation:

$$\lambda'(t;\Delta t) = 2R_G(t;\Delta t) \qquad (5)$$

The prefactor of 2 has been introduced in order to correctly account for the whole area covered by the swarm of points. Diffusion jumps are obviously not absolutely sharp but rather complicated events, and therefore, the means to describe them should reflect this fact. In this respect, if the time interval Δt is long enough, the respective set of successive positions constitutes a random walk. This assumption has indeed been confirmed by plotting the average square length $\lambda'^2(t;\Delta t)$ with time interval Δt, which yielded a straight line.[45] Then, the positions recorded within each time interval constitute a normal distribution centered at $\mathbf{R}_{CM}$ (eq 4), with a standard deviation equal to the radius of gyration (eq 3). The standard deviation of a normal distribution multiplied by 2 is a common measure for its width and therefore constitutes a plausible choice for our definition of the diffusion jump length.

As a simpler variant of the above method, one could use the measure of the observation points swarm end-to-end vector,

$$r_{1N}(t;\Delta t) = ||\mathbf{R}_1(t;\Delta t) - \mathbf{R}_N(t;\Delta t)|| \qquad (6)$$

to describe its size with time. This is useful in estimating the size of diffusion jumps, but as our experience showed, it results in a much noisier signal and therefore is not practical. On the contrary, the radius of gyration time series, $R_G(t;\Delta t)$, leads to a smoother curve, which allows one to precisely identify jumps with peaks in the respective graph. Moreover, it can reliably estimate a jump's size since R_G, as given by eq 3, is an appropriate measure of the extent to which the successive penetrant positions are spread in space over a certain time period. It should be also noted that the method introduced in this work manages to isolate the jumps mechanism from other processes also underlying diffusion, as, for instance, smooth translation, revealing the real extent of its contribution. Finally, a refinement introduced in the next paragraphs will allow us to incorporate the quantity defined by eq 6, in an appropriate factor multiplying the length introduced in eq 5, so as to correctly determine the successful jumps contribution to the overall diffusive displacement.

Indeed, by considering the series of jumps observed as a random walk, one can define a corresponding diffusion coefficient, $D_{s,\ jumps}$, via the well-known formula:[51]

$$D_{s,\ jumps} = \frac{1}{6}\nu\lambda^2 \qquad (7)$$

where ν denotes the frequency of successful jumps and λ denotes the average jump length. In terms of simulation results, the frequency ν is calculated as the number of all successful jumps performed by all of the penetrants divided by the total simulation time. The diffusion coefficient $D_{s,\ jumps}$ provides the measure of jumps contribution to the overall diffusive motion.

At this point, we should discuss two problems. The first one is related to the arbitrary parameter Δt entering the jump length definition by eq 5 and how one could remove it. The second problem concerns the question of how to distinguish between successful and unsuccessful jumps so as to calculate a reliable $D_{s,\ jumps}$ via eq 7. These two problems are solved simultaneously according to the following argumentation: An ideal successful jump could be considered as that of a molecule moving along a straight line from the first to the last of a set of N consecutive points. In real situations, however, the penetrant should follow a much more complicated trajectory between the first and the last point, more or less deviating from ideality. Therefore, the ratio of the distance r_{1N} divided by the contour length of the particle's real path from point 1 to N should provide a measure of such deviations. In the extreme case of a penetrant returning to its initial host cavity, r_{1N} would be close to zero and so would the ideality ratio. This kind of event can be considered as an unsuccessful jump. Consequently, one may use this ratio to properly weight the jump size curve obtained by eq 5. Obviously, the sum of the distances $r_{i,i+1}$, $i = 1, 2, ..., N - 1$, would replace the contour length of the penetrant path, leading to a reformulated definition of jump length replacing that of eq 5, in the following manner:

$$\lambda(t) = 2R_G(t;\Delta t)\frac{||\mathbf{R}_1(t;\Delta t) - \mathbf{R}_N(t;\Delta t)||}{\sum_{i=1}^{N-1}||\mathbf{R}_i(t;\Delta t) - \mathbf{R}_{i+1}(t;\Delta t)||} \qquad (8)$$

Moreover, the average of the above quantity over the total simulation time and all of the penetrants in the system can be easily shown to be essentially independent of the time interval Δt (see Appendix B), a fact that has been also confirmed by our results, as will be explained in the subsequent section 3. This way, the arbitrary parameter problem is also eliminated.

By comparing the random walk diffusion coefficient, $D_{s,\ jumps}$, based on the weighted jump length $\lambda(t)$ to the one directly obtained from the mean square displacement (MSD) relation with time scales, $D_{s,\ MSD}$, one can estimate the contribution of jumps to the overall diffusive motion. In particular, we may state that the jumps contribution to the diffusive motion is important if the respective random walk diffusivity is close to the mean square displacement one. If, on the other hand, the former is, for example, 1 order of magnitude lower than the latter, additional diffusion mechanisms such as smooth translation of the reptation kind should be present.

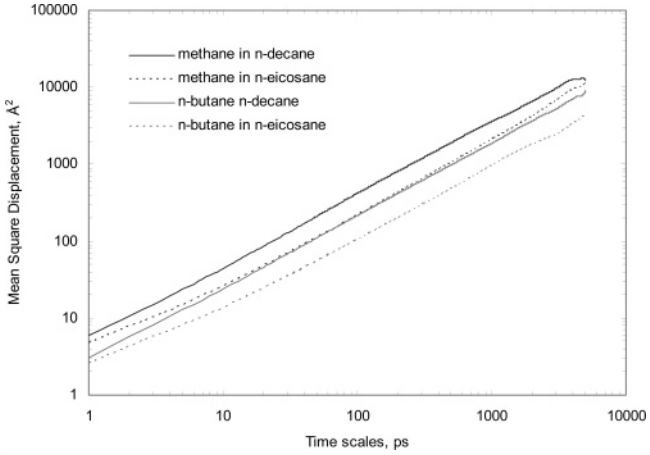

Figure 2. Mean square displacement (Å^2) of methane and *n*-butane dispersed in *n*-decane and *n*-eicosane.

One more final remark should be added concerning the validity of treating jumps as a random walk process to discern whether they coexist or not with other factors causing diffusion. It is well-known that, although jumps are random events, their randomness, justifying use of eq 7, is clearly exhibited only beyond a certain space−time scale,[31] which depends on the particular system under study. Otherwise, subdiffusion is observed because of the restrictions imposed upon penetrants by the surrounding matrix molecules. Nevertheless, if the overall diffusion *is* in the normal regime, then two possible cases exist: either the jumps themselves constitute a subdiffusive process and consequently can not be the sole contribution to the mass transport process, or they do constitute a true three-dimensional random walk, and then it is fair to use the respective formalism combined with our jumps analysis to decide whether they are the only important microscopic diffusion mechanism or not.

3. Results and Discussion

3.1. Macroscopic Mass Transport Properties. First, the gaseous alkanes self-diffusion coefficients, $D_{s,\,MSD}$, were calculated from the well-known Einstein relation connecting mean square displacement with time scales

$$D_{s,MSD} = \lim_{\tau\to\infty} \frac{1}{6\tau} \langle |\mathbf{R}_i(t_0+\tau) - \mathbf{R}_i(t_0)|^2 \rangle_{i,t_0} \qquad (9)$$

where τ is the time scale and $\mathbf{R}_i(t)$ is the position vector for the center of mass of molecule i at time t. The brackets $\langle\ \rangle_{i,t_0}$ denote averaging with respect to all molecules i of a given type, gas or liquid, and all initial times t_0 of every time scale τ. The quantity $\langle |\mathbf{R}_i(t_0+\tau) - \mathbf{R}_i(t_0)|^2 \rangle_{i,t_0}$ is the mean square displacement (MSD) of the diffusing molecule. Results for methane and *n*-butane in *n*-decane and *n*-eicosane are shown in Figure 2. Similar curves have been obtained for all of the other systems studied in this work. From the curves in Figure 2, we easily observe that a linear part is clearly present which allows one to define self-diffusivity according to eq 9. Table 2 summarizes self-diffusion coefficient values of all gas−liquid mixtures obtained from present simulations. At this point, it is worth noting the remarkable deviation of methane's diffusivity observed in the presence of *n*-butane with respect to the one calculated for pure methane.

The values of the displacement correlation matrix elements, normalized by the MSD, have also been computed to infer about the possible anisotropy in the penetrants' motion. These are defined by

$$C_{\alpha\beta}(\tau) = \frac{\langle \Delta\alpha_i \Delta\beta_i \rangle_{i,t_0}}{\langle \Delta R_i^{\,2} \rangle_{i,t_0}} - \frac{\delta_{\alpha\beta}}{3} \qquad (10)$$

where $\Delta R_i = |\mathbf{R}_i(t_0+\tau) - \mathbf{R}_i(t_0)|$, $\Delta\alpha_i = |\alpha_i(t_0+\tau) - \alpha_i(t_0)|$ with $\alpha = x, y, z$, and $\delta_{\alpha\beta}$ is Kronecker's symbol, so that the condition for isotropic diffusion assumes the following particularly simple form:

$$\lim_{\tau\to\infty} C_{\alpha\beta}(\tau) = 0 \qquad (11)$$

In Table 2, the average values over diagonal, $\alpha = \beta$, and nondiagonal, $\alpha \neq \beta$, elements and over time scales from 1000 up to 4000 ps are shown, together with the diffusion coefficients. Time scales shorter than 1000 ps were excluded so as to fulfill the condition for long τ, eq 11, whereas the ones longer than 4000 ps were rejected as subject to larger statistical error as the respective time intervals become fewer. The obtained values show that there is neither significant anisotropy nor any strong correlation in the penetrants' motion along the *x*, *y*, or *z* axis in any of the systems studied. This result together with the form of the curves in Figure 2 imply that normal diffusion has been attained within the space and time scales studied.

The MSD based self-diffusion coefficients are also shown graphically in Figure 3 as a function of carbon atoms in the penetrant molecule. The results presented in this subsection provide valuable information about the dependence of systems' mass transport properties on such parameters as penetrant or matrix molecular weight. However, no direct information about the underlying diffusion mechanism can be acquired. It should be noted also, that the obtained Einstein or MSD coefficients constitute a measure of the *overall* diffusive motion of the penetrants; in other words, they incorporate contributions from all microscopic mechanisms that possibly act in the systems. In the next subsection, we proceed to the investigation of microscopic molecular motion via the new jumps detection technique.

TABLE 2: Self-Diffusion Coefficients, $D_s \times 10^7$ cm^2 s^{-1}, of Gaseous Alkanes Dispersed in Normal Alkane "Heavy Substances", $n-C_nH_{2n+2}$, at 293.15 K Temperature and Normal Pressure, with Respect to Degree of Polymerization, *n*, and Elements of the Displacement Correlation Matrix Averaged over Diagonal or Nondiagonal Terms and Time Scales (See Main Text, Section 3.1, for Details)

	penetrant:	methane	ethane	propane	*n*-butane	methane (mixed with *n*-butane)	*n*-butane (mixed with methane)
n-decane	$D_s \times 10^6$ cm^2 s^{-1} in *n*-decane	55	44	42	30	87	29
	$\langle C_{\alpha\alpha}(\tau)\rangle_{a,\tau}$	0.00 ± 0.03	0.00 ± 0.08	0.00 ± 0.04	0.00 ± 0.05	0.00 ± 0.07	0.00 ± 0.06
	$\langle C_{\alpha\beta}(\tau)\rangle_{a,\beta,\tau}$	−0.01 ± 0.04	−0.04 ± 0.02	0.02 ± 0.04	0.04 ± 0.03	−0.02 ± 0.07	−0.04 ± 0.06
n-eicosane	$D_s \times 10^6$ cm^2 s^{-1} in *n*-eicosane	36	22	19	14	29	23
	$\langle C_{\alpha\alpha}(\tau)\rangle_{a,\tau}$	0.00 ± 0.04	0.00 ± 0.04	0.00 ± 0.11	0.00 ± 0.04	0.00 ± 0.04	0.00 ± 0.03
	$\langle C_{\alpha\beta}(\tau)\rangle_{a,\beta,\tau}$	0.00 ± 0.03	0.02 ± 0.02	0.03 ± 0.06	−0.02 ± 0.02	0.01 ± 0.07	−0.05 ± 0.08

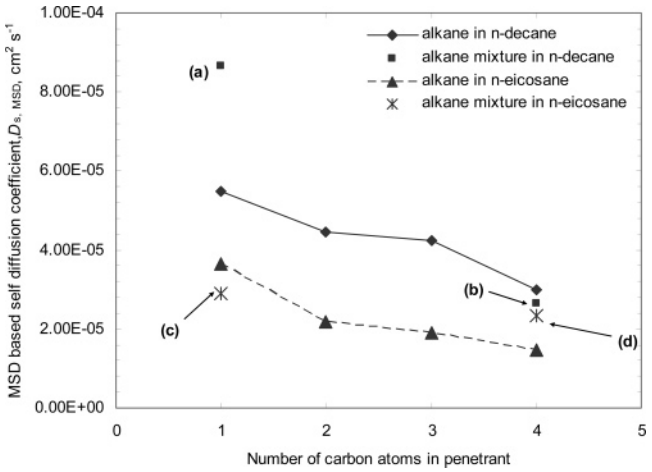

Figure 3. Self-diffusion coefficients of alkane gases, in square centimeters per second, based on MSD data. For the purpose of clarity, values corresponding to gas mixtures are also labeled in the following manner: (a) methane (mixed with *n*-butane) in *n*-decane, (b) *n*-butane (mixed with methane) in *n*-decane (c) methane (mixed with *n*-butane) in *n*-eicosane, (d) *n*-butane (mixed with methane) in *n*-eicosane.

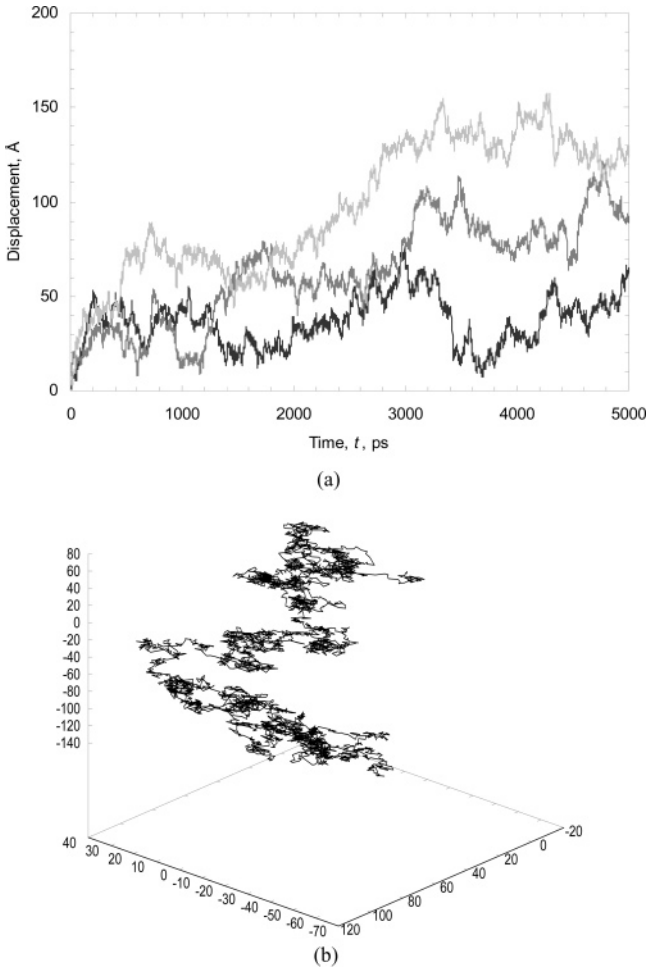

Figure 4. (a) Displacement $\Delta R_i(t) = ||\mathbf{R}_i(t) - \mathbf{R}_i(0)||$ of three methane molecules diffusing in *n*-decane. (b) Trajectory of one of the above methane molecules (periodic boundary conditions removed).

3.2. Microscopic Diffusion Mechanisms. Before proceeding to the application of our method, we depict the penetrants' behavior in terms of a displacement with time graph, Figure 4a, and a three-dimensional plot, Figure 4b, for a representative case of a single methane molecule diffusing in *n*-decane. The noisy or "blurred" nature of the trajectory is evident in these pictures. As will be explained in the next paragraph, this fact is connected to the coexistence of the jump mechanism with other microscopic contributions to the overall diffusion, a fact related to the "softness" of the liquid alkane matrices chosen in this work. It should also be noted, with respect to Figure 4b, that, although jumps between distinct regions are observed, clearly, they are not the sole contributors to the overall diffusion.

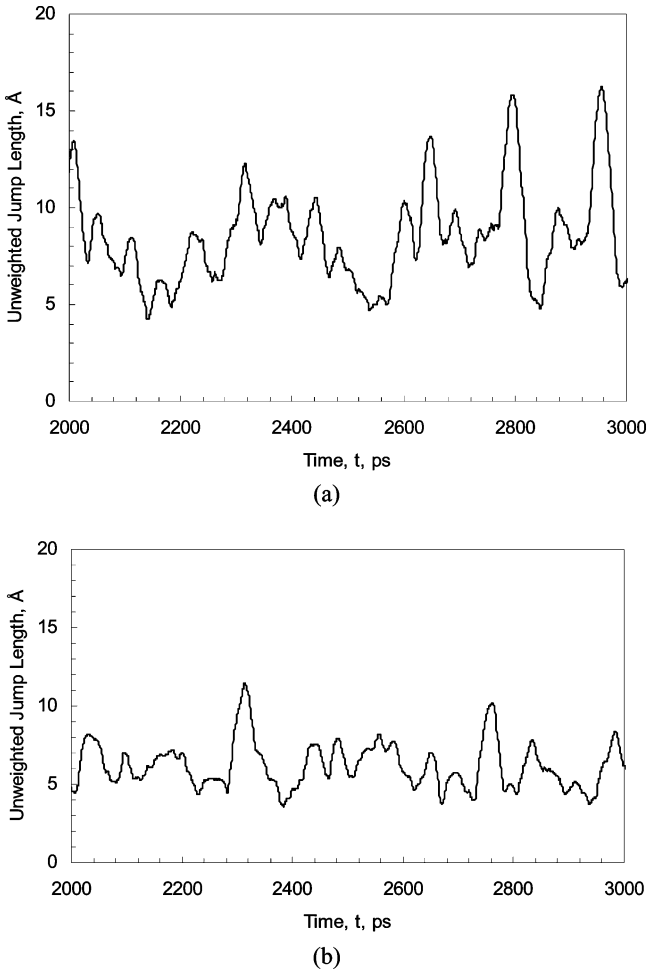

Figure 5. (a) Identification of jumps of a single methane molecule diffusing through *n*-decane via the "unweighted" version of our method, eqs 3 and 5. (b) Same as in (a), for a *n*-butane molecule.

In applying our method, the unweighted jump length definition, given by eqs 3 and 5, was employed first. Thus, we obtain a picture of the penetrants mobility, regardless of the jumps real contribution to the overall diffusion. Figure 5a,b shows individual unweighted jump graphs for single methane and *n*-butane molecules in *n*-decane for a given time interval Δt. It is evident that heavier *n*-butane molecules tend to perform shorter jumps than methane ones. In order to proceed further, quantitatively, we need to isolate the local maxima of each curve, which we identify with jump events, and record their values. Then, we can process these data statistically, as will be shown in the next paragraphs. Usually, the curves obtained are smooth enough that their maxima can be located by simply tracking the change in slope, expressed as the difference between two successive recorded values. In some cases, however, an amount of "residual" noise was still present and had to be removed by employing moving averages over 10−20 successive points.

As mentioned above, jump lengths should be properly weighted to account for unsuccessful jumps, that is, jump events

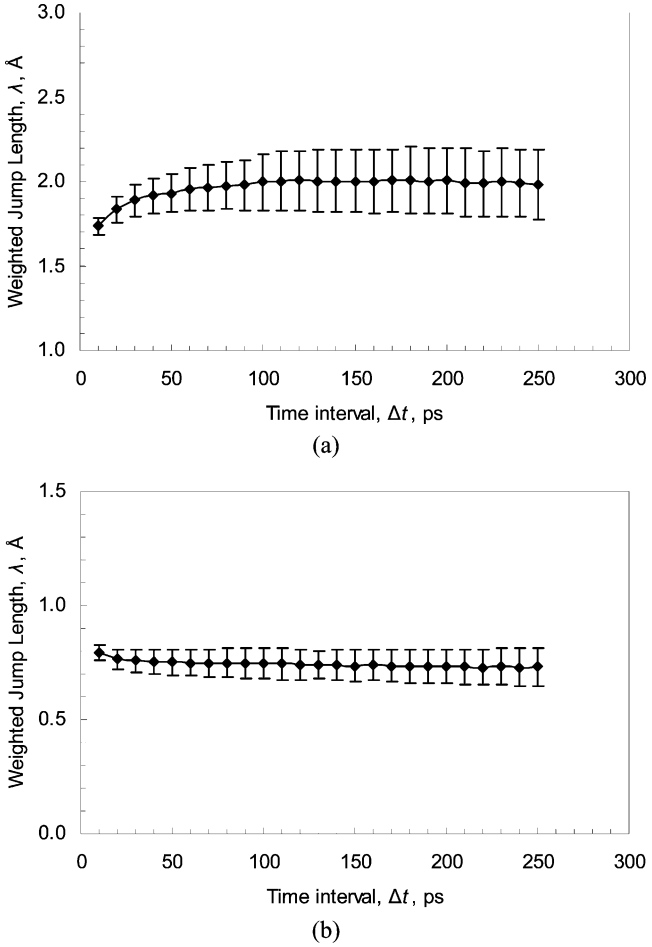

Figure 6. (a) Weighted jump length, λ, for methane in *n*-decane versus time interval Δt. Its value attains an asymptotic limit for large enough Δt. (b) Same as in (a) for *n*-butane in *n*-eicosane.

that do not result in substantial translocation of the penetrant. Essentially, this leads to the calculation of effective jump lengths, which are usually substantially smaller than the unweighted ones, as our calculations showed. The weighting scheme proposed here is also shown to remove the arbitrariness inherent in employing a time window Δt. This is corroborated by the results depicted in Figure 6a,b showing the weighted jump length for methane and *n*-butane reaching an asymptotic value as predicted theoretically (Appendix B). Similar curves have been obtained in all other cases studied here. At this point, we should also note that all local maxima identified in our plots were taken into account in our subsequent analysis. Indeed, calculation of R_G essentially leads to smoothing out fluctuations that should not be considered as jumps, especially for large Δt. However, in some cases, calculations were repeated by employing only the part of the unweighted jumps curve with values larger than the penetration length $(D_{MSD}\Delta t)^{1/2}$, in determining the weighted lengths. The difference in the average length and jump induced diffusion coefficients between filtering and nonfiltering computations was insignificant.

Figure 7 shows the dependence of penetrant weighted jump length on molecular weights. It is observed that jump length tends to smaller values with increasing penetrant or matrix molecular weight. However, the dependence on penetrant molecular weight is remarkably weak, especially in the case of diffusion through *n*-eicosane. An interpretation of this finding will be attempted in the next paragraphs. It should be noted that the weighting scheme introduced by eq 8 represents an effective average length or, in other words, a measure of the

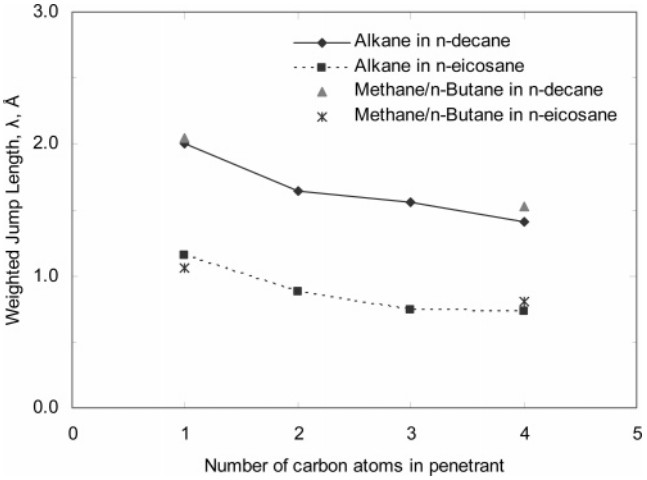

Figure 7. Dependence of weighted jump length, eq 8, on penetrant molecular weight.

jumps contribution to the overall diffusivity and not the jumps' actual size. The latter is given, of course, by the radius of gyration, eq 5. The small values shown in Figures 6 and 7 suggest that the jumps contribution to the overall penetrant diffusive motion is small in the case of the systems studied.

In Figure 8, the MSD or Einstein self-diffusion coefficient, $D_{s,MSD}$ is compared to the $D_{s,jumps}$ value based on weighted jumps for all gas species in *n*-decane and *n*-eicosane. The notable conclusion is that jump lengths and resulting jump induced diffusivities are less sensitive to molecular weight dependence than MSD coefficients. In addition, jump induced diffusivities are much lower than the MSD one, leading to the unavoidable conclusion that the jumps mechanism has a low contribution to the overall diffusive motion in the systems studied in this work. This is not surprising since the *n*-decane and *n*-eicosane chains are not long enough to reach the entanglement limit and form a more or less stable matrix with persistent free volume cavities. The environment in which penetrants move changes more rapidly than it would in the case of matrices made of high molecular weight chains with very long relaxation times. Therefore, in the systems studied here, diffusion preserves some characteristics of mass transport phenomena observed in simpler, low molecular weight liquids.

However, as Figure 7 shows, passing from *n*-decane to *n*-eicosane, jump length tends to be unaffected by penetrant molecular weight. This is an indication that, in the latter case, occurrence of jump events is mainly affected by the matrix microstructure and to a much lesser degree by the penetrant molecular weight. In other words, the *n*-eicosane matrix is a much less mobile system,[45] and long-lived free volume cavities are formed in it. Therefore, jump events are limited to translocations among "well-defined" cavities as has been observed in previous simulation studies, and jump length mostly depends on the distances between such cavities rather than on the penetrant mobility. Finally, it should be noted that a fairly constant ratio of MSD over jump induced diffusivity has been observed. Its values are 10.0 ± 1.0 Å in *n*-decane and 17.5 ± 2.0 Å in *n*-eicosane.

From all of the above remarks and observations, we may form a more concrete picture of the microscopic mechanisms underlying gas diffusion in the matrices herein studied, *n*-decane and *n*-eicosane. In *n*-decane, a more liquid-like transportation mechanism prevails, which might include smooth translation and to a small extent jumps to temporarily formed cavities. In

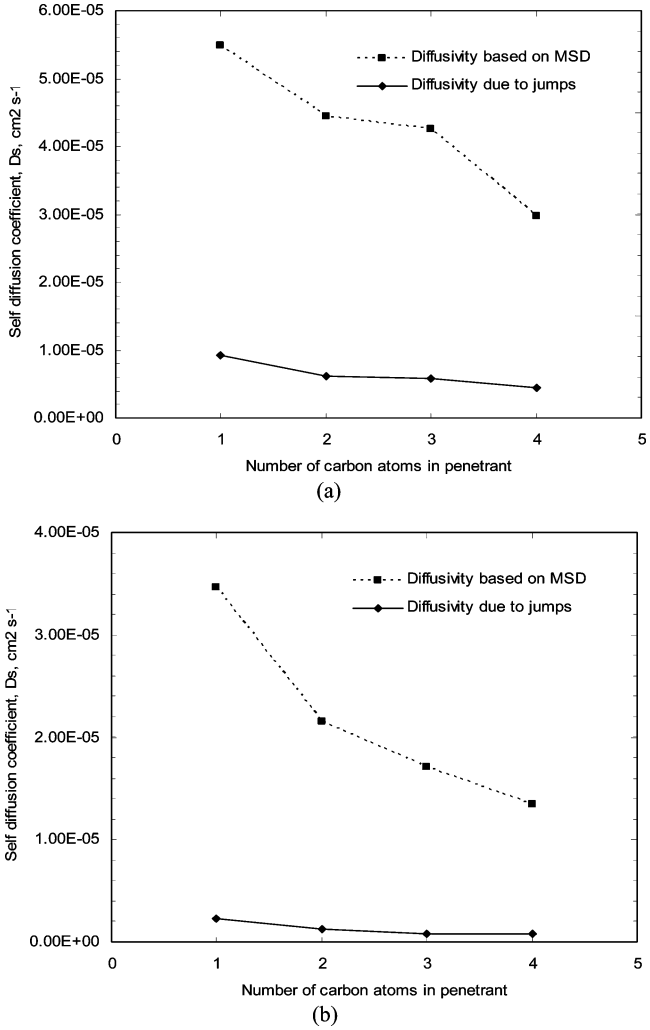

Figure 8. Self-diffusion coefficient based on weighted jump lengths and frequencies compared to values based on MSD (Einstein relation), for (a) *n*-decane and (b) *n*-eicosane systems.

n-eicosane, smooth translation is inhibited, but so are the penetrant jumps. This is probably because jumps in this case, are only possible among long-lived cavities that are formed in the matrix. In other words, opening and closing of temporary cavities is less frequent, and therefore chances for a penetrant to jump into them are also reduced. In *n*-eicosane, smooth translation is still possible and indeed constitutes the main contribution to the overall diffusion. If we moved to higher molecular weight matrices however, intercavity jumps would probably be the main mechanism. Then, assuming that free volume distribution is more or less similar to that of *n*-eicosane, diffusion coefficients in high polymer matrices might be of the order of $D_{s,jumps}$ values herein calculated. This consideration is not inconsistent with already published results concerning the flow of gaseous alkanes through poly(ethylene).[52] However, a definite confirmation of this assumption will be given by further analysis of simulation results concerning polymer simulation via the jumps detection method.

4. General Discussion and Concluding Remarks

In this work, a method was presented for identifying individual penetrant jump events that take place in the course of molecular dynamics simulations. In contrast with previous attempts, the method is able to directly identify each individual jump event, and assign it a measure proposed by us. These data can be easily collected and further processed statistically (average jump length, length distribution, etc.), leading to conclusions about the characteristics of jumps and about their contribution to the mass transport processes that take place. This way, one can discern whether diffusion of penetrants in the system is mainly due to such jump events or other microscopic mechanisms also present. It should be noted that the method is based on analyzing the penetrants' trajectories in space and not the surrounding matrix motion. Therefore, all jumps are identified regardless of their origin. For instance, the matrix itself might impose a penetrant's translocation through some kind of collective rearrangement. Although such a behavior has been identified as the cause of smooth rather than sharp penetrant displacements,[32] we should not exclude the possibility of "matrix induced" jumps.

The method was applied in systems of *n*-decane and *n*-eicosane with gaseous normal alkanes dispersed therein. Our results suggest that diffusive jumps are not the only mechanism present in such systems. On the contrary, other mechanisms such as gradual translation play a more important role in the specific systems. On the other hand, the average jump length is a weak function of penetrant molecular weight in the case of *n*-eicosane, which suggests that, in those systems, diffusion jumps are more or less a matter of free volume distribution. In other words, as the matrix molecular weight increases, free volume cavities as well as their distribution become more persistent with time and impose a corresponding distribution of possible jump lengths.

Appendix A

Determination of "Local" mNT Parameters. In both the UA−TraPPE force-field[44] and the NERD model,[43] nonbonded interactions comprise intramolecular pairs of interaction centers separated by four or more bonds, while the torsion potential affects atoms separated by three bonds and has a dependency on the torsion angle φ, of the form:

$$V_{\phi,\mathrm{TraPPE}} = V_0 + V_1(1 + \cos\phi) + V_2(1 - \cos 2\phi) + V_3(1 + \cos 3\phi) \quad (12)$$

In our mNT model, the total torsion energy is a sum of (i) an intrinsic torsion potential, eq 1, characterizing every bond, and (ii) nonbonded interactions, eq 2 between interaction centers separated by three of four bonds, which are referred to as "local" in contrast to the remaining nonbonded "nonlocal" interactions. Simulations based on this distinction have already been successfully conducted in the case of polypropylene[53] and organosilicon polymers.[54−56]

For the case of the simplest alkane with a rotating bond in the main chain, *n*-butane, we require this sum to approximate the torsion potential predicted by NERD/TraPPE. Butane is chosen because of both simplicity of the problem and absence of nonbonded intramolecular forces in its NERD/TraPPE representation. First, we choose a pair diameter σ such that the distance of end methyl groups in the trans configuration minimizes the corresponding Lennard-Jones potential, that is

$$r^{\mathrm{trans}}_{\mathrm{CH_3-CH_3}} = 2^{1/6}\sigma \quad (13)$$

Then, we choose depth ϵ and torsion potential barrier k_φ so as to minimize the square error between NERD/TraPPE and mNT:

$$\sum_{\phi}\left(V_{\phi,\,\mathrm{TraPPE}}-\underbrace{\left(V_{\mathrm{nb,\,local}}+\frac{1}{2}k_{\phi}\left(1+\cos 3\phi\right)\right)}_{\text{mNT effective torsion potential}}+\varepsilon_{\mathrm{local}}\right)^{2} \quad (14)$$

the angle φ varying from 0 to 360° with a step of 1°. The potential shift by ϵ does not affect the molecular dynamics which is solely based on energy variations rather than its absolute values.

Given a torsion potential barrier, the smallest distance of the methyl groups $r = r^{\mathrm{cis}}_{\mathrm{CH_3-CH_3}}$ observed in a cis configuration should maximize

$$\Delta V_{\mathrm{nb,local}} = V_{\phi,\mathrm{TraPPE}} - \frac{1}{2}k_{\phi}(1+\cos 3\phi) + \epsilon_{\mathrm{local}} \quad (15)$$

Therefore, it holds that

$$\epsilon = \Delta V_{\max}\left(\frac{r}{\sigma}\right)^{6}/4\left(\left(\frac{\sigma}{r}\right)^{6}-1\right) \quad (16)$$

Finally, the torsion potential barrier, k_{φ}, is determined so as to minimize the square error in eq 14, which was computed to be 12.7%.[45]

Appendix B

Asymptotic Limit of the Average Weighted Jump Length. According to eq 8, the average weighted jump length is equal to

$$\langle\lambda\rangle = 2\langle R_{\mathrm{G}}(t;\Delta t)||\mathbf{R}_1-\mathbf{R}_N||/\sum_{i=1}^{N-1}||\mathbf{R}_i-\mathbf{R}_{i+1}||\rangle \quad (17)$$

Assuming diffusive motion implies that, for large enough Δt,

$$\langle|\mathbf{R}_1-\mathbf{R}_N|\rangle \propto \Delta t^{1/2} \quad (18)$$

which is a reformulation of the Einstein relation, eq 9. In a similar fashion,

$$\langle R_{\mathrm{G}}(t;\Delta t)\rangle \propto \Delta t^{1/2} \quad (19)$$

expresses the connection of the standard deviation of positions' distribution with elapsed time, characterizing random walks in general. Besides, the denominator in eq 17 should be proportional to Δt:

$$\sum_{i=1}^{N-1}||\mathbf{R}_i-\mathbf{R}_{i+1}|| \propto N = \Delta t/\delta t \quad (20)$$

with δt denoting the time interval between two successive positions $\mathbf{R}_i$ and $\mathbf{R}_{i+1}$. The last three equations imply that

$$\langle\lambda\rangle = 2\langle(\epsilon\Delta t^{1/2}+\epsilon'(\Delta t))(\zeta\Delta t^{1/2}+\zeta'(\Delta t))/(\eta\Delta t+\eta'(\Delta t))\rangle \quad (21)$$

with κ, λ, and μ as constants and $\langle\epsilon'(\Delta t)\rangle/\Delta t^{1/2}$, $\langle\zeta'(\Delta t)\rangle/\Delta t^{1/2}$, $\langle\eta'(\Delta t)\rangle/\Delta t \rightarrow 0$, leading to

$$\langle\lambda\rangle \rightarrow 2\epsilon\zeta/\eta = \text{constant} \quad (22)$$

for $\Delta t \rightarrow \infty$. In the case of systems where long jumps are frequently observed, two possible scenaria may be anticipated: In the first one, the penetrant motion reduces to a quasi-one-dimensional random walk, and the above derivation is still valid. In the second scenario, considerable deviations off a pure random walk might show up as the penetrant tends to move ballistically rather than erratically. Then, the quantities in eqs 18 and 19 will be proportional to Δt rather than to its square root. Equation 20 is still expected to hold since, in that case, $\sum_{i=1}^{N-1}||\mathbf{R}_i-\mathbf{R}_{i+1}|| \approx ||\mathbf{R}_1-\mathbf{R}_N||$. In other words, a penetrant moving in a channel connecting two adjacent cavities will be subjected to friction forces that will prevent it from accelerating. Then, a dependence on Δt could be observed for intermediate Δt values. As we move on to longer time intervals, the overall intercavity motion again reduces to a random walk, and any dependence on Δt should disappear. In fact, the threshold at which the average weighted jump length becomes constant should provide an indication of the average jump duration.

Note Added after ASAP Publication. This article was published ASAP on Nov 1, 2007. A Supporting Information paragraph was added. The corrected version was reposted on Nov 6, 2007.

Supporting Information Available: Torsional potential herein employed with respect to torsion angle, as compared with TraPPE and sinusoidal potentials; evidence proving sufficient equilibration of the structures simulated, in the form of bond angles distribution, time autocorrelation function of the end-to-end vector of the chain molecules and time autocorrelation of dihedral angles; and average square of unweighted jump length with respect to varying time intervals Δt. This material is available free of charge via the Internet at http://pubs.acs.org.

References and Notes

(1) Tyrell, H. J. V.; Harris, K. R. *Diffusion in Liquids;* Butterworths: London, 1984. (b) Ricci, F. P.; Rocca, D. Diffusion in Liquids. In *Molecular Liquids: Dynamics and Interactions;* Barnes, A. J., Orville-Thomas, W. J., Yarwood, J., Eds.; NATO ASI: Dordrecht, Holland, 1984; Vol C 135, pp 35−58.
(2) Riekert, L. *AIChE J.* **1971**, *17*, 446.
(3) Kärger, J. *J. Phys. Chem.* **1981**, *95*, 5558.
(4) Reed, D. A.; Ehrich, G. *Surf. Sci.* **1981**, *102*, 588.
(5) Reed, D. A.; Ehrich, G. *Surf. Sci.* **1981**, *105*, 603.
(6) Sundaram, N.; Yang, R. T. *Chem. Eng. Sci.* **2000**, *55*, 1747.
(7) Paschek, D.; Krishna, R. *Chem. Phys. Lett.* **2001**, *342*, 148.
(8) Krishna, R.; Paschek, D. *Chem. Eng. J.* **2002**, *87*, 1.
(9) Ikeda-Fukazawa, T.; Kawamura, K.; Hondoh, T. *Mol. Sim.* **2004**, *30*, 973.
(10) Bendani, A.; Dautant, A.; Bonpunt, L. *J. Phys. I France* **1993**, *3*, 887.
(11) Sevick, E. M.; Bell, A. T.; Theodorou, D. N. *J. Chem. Phys.* **1993**, *98*, 3196.
(12) June, R. L.; Bell, A. T.; Theodorou, D. N. *J. Phys. Chem.* **1991**, *95*, 8866.
(13) Snurr, R. Q.; Bell, A. T.; Theodorou, D. N. *J. Phys. Chem.* **1994**, *98*, 11948.
(14) Maginn, E. J.; Bell, A. T.; Theodorou, D. N. *J. Phys. Chem.* **1996**, *100*, 7155.
(15) Greenfield, M. L.; Theodorou, D. N. *Macromolecules* **1998**, *31*, 7068.
(16) Theodorou, D. N.; Wei, J. *J. Catal.* **1990**, *83*, 205.
(17) Maginn, E. J.; Bell, A. T.; Theodorou, D. N. *J. Phys. Chem.* **1993**, *97*, 4173.
(18) Gaub, M.; Fritzsche, S.; Haberlandt, R.; Theodorou, D. N. *J. Phys. Chem. B* **1999**, *103*, 4721.
(19) Karayiannis, N. C.; Mavrantzas, V. G.; Theodorou, D. N. *Chem. Eng. Sci.* **2001**, *56*, 2789.
(20) Sonnenburg, J.; Gao, J.; Weiner, J. H. *Macromolecules* **1990**, *23*, 4653.
(21) Takeuchi, H. *J. Chem. Phys.* **1990**, *93*, 2062.
(22) Takeuchi, H. *J. Chem. Phys.* **1990**, *93*, 4490.
(23) Müller-Plathe, F.; Rogers, S. C.; van Gunsteren, W. F. *Chem. Phys. Lett.* **1992**, *199*, 237.
(24) Müller-Plathe, F. *J. Chem. Phys.* **1991**, *94*, 3192.
(25) Müller-Plathe, F. *J. Chem. Phys.* **1992**, *96*, 3200.
(26) Sok, R. M.; Berendsen, H. J. C.; van Gunsteren, W. F. *J. Chem. Phys.* **1992**, *96*, 4699.

(27) Pant, P. V. K.; Boyd, R. H. *Macromolecules* **1993**, *26*, 679.
(28) Gusev, A. A.; Müller-Plathe, F.; van Gunsteren, W. R.; Suter, U. W. *Adv. Polym. Sci.* **1994**, *116*, 207.
(29) Takeuchi, H.; Okazaki, K. *Kobunshi Ronbunshu* **1994**, *51*, 387.
(30) Chassapis, C. S.; Petrou, J. K.; Petropoulos, J. H.; Theodorou, D. N. *Macromolecules* **1996**, *29*, 3615.
(31) Müller-Plathe, F. *J. Membr. Sci.* **1998**, *141*, 147.
(32) Hahn, O.; Mooney, D. A.; Müller-Plathe, F.; Kremer, K. *J. Chem. Phys.* **1999**, *111*, 6061.
(33) Mooney, D. A.; MacElroy, J. M. D. *J. Chem. Phys.* **1999**, *110*, 11087.
(34) Tocci, E.; Hofmann, D.; Paul, D.; Russo, N.; Drioli, E. *Polymer* **2001**, *42*, 521.
(35) Neyertz, S.; Brown, D. *Macromolecules* **2004**, *37*, 10109.
(36) Pavel, D.; Shanks, R. *Polymer* **2005**, *46*, 6135.
(37) Striolo, A.; McCabe, C.; Cummings, P. T. *Macromolecules* **2005**, *38*, 8950.
(38) Striolo, A.; McCabe, C.; Cummings, P. T. *J. Phys. Chem. B* **2005**, *109*, 14300.
(39) Meunier, M. *J. Chem. Phys.* **2005**, *123*, 134906.
(40) Tung, K. L.; Lu, K. T. *J. Membr. Sci.* **2006**, *272*, 37.
(41) Smit, E.; Mulder, M. H. V.; Smolders, C. A.; Karrenbeld, H.; van Eerden, J.; Feil, D. *J. Membr. Sci.* **1992**, *73*, 247.
(42) Chang, R.; Yethiraj, A. *Phys. Rev. Lett.* **2006**, *96*, 107802.
(43) Nath, S. K.; Escobedo, F. A.; de Pablo, J. J. *J. Chem. Phys.* **1998**, *108*, 9905.
(44) Martin, M. G.; Siepmann, J. I. *J. Phys. Chem. B* **1998**, *102*, 2569.
(45) The reader may also review the supporting information material provided at this journal's website.
(46) Lide, D. R., Ed. *Handbook of Chemistry and Physics;* CRC Press: Boca Raton, FL, 1998−1999; 79th ed.
(47) Gear, C. W., *Numerical initial value problems in ordinary differential equations*; Prentice Hall: Englewood Cliffs, 1971.
(48) Verlet, L. *Phys. Rev.* **1967**, *159*, 98.
(49) Nosé, S.; Klein, M. L. *Mol. Phys.* **1983**, *50*, 1055.
(50) Theodorou, D. N.; Boone, T. D.; Dodd, L. R.; Mansfield, K. F. *Makromol. Chem. Theory Simul.* **1993**, *2*, 191.
(51) Chandrasekhar, S. *Rev. Mod. Phys.* **1943**, *15*, 1.
(52) Michaels, A. S.; Bixler, H. J. *J. Polym. Sci.* **1961**, *10*, 413.
(53) Antoniadis, S. J.; Samara, C. T.; Theodorou, D. N. *Macromolecules* **1998**, *22*, 7944.
(54) Raptis, V. E.; Economou, I. G.; Theodorou, D. N.; Petrou, J.; Petropoulos, J. H. *Macromolecules* **2004**, *37*, 1102.
(55) Makrodimitri, Z. A.; Raptis, V. E.; Economou, I. G. *J. Phys. Chem. B* **2006**, *110*, 16047.
(56) Makrodimitri, Z. A.; V. E.; Economou, I. G. *Macromolecules* **2007**, *40*, 1720.